frontiers | Frontiers in Physics

TYPE Brief Research Report
PUBLISHED 29 March 2023
DOI 10.3389/fphy.2023.1149337



OPEN ACCESS

EDITED BY
Zhangqi Yin,
Beijing Institute of Technology, China

REVIEWED BY
Keyu Xia,
Nanjing University, China
Jiteng Sheng,
East China Normal University, China

*CORRESPONDENCE
Hao Fu,
h.fu@live.cn

†These authors contributed equally to this work

SPECIALTY SECTION
This article was submitted to Optics and Photonics, a section of the journal Frontiers in Physics

RECEIVED 21 January 2023
ACCEPTED 13 March 2023
PUBLISHED 29 March 2023

CITATION
Gong Z-C, Shen C-Y, Yuan Q, Sun C-P, Li Y and Fu H (2023), Sympathetic feedback cooling in the optomechanical system consisting of two coupled cantilevers.
*Front. Phys.* 11:1149337.
doi: 10.3389/fphy.2023.1149337



# Sympathetic feedback cooling in the optomechanical system consisting of two coupled cantilevers

Zhi-Cheng Gong[1,2†], Cheng-Yu Shen[2,3†], Quan Yuan[2,3], Chang-Pu Sun[4,5], Yong Li[1,6] and Hao Fu[1,2*]

[1]School of Science, Hainan University, Haikou, China, [2]Innovation Academy for Precision Measurement Science and Technology, Chinese Academy of Sciences, Wuhan, China, [3]University of Chinese Academy of Science, Beijing, China, [4]Graduate School of China Academy of Engineering Physics, Beijing, China, [5]Beijing Computational Science Research Center, Beijing, China, [6]Center for Theoretical Physics, Hainan University, Haikou, China

We present sympathetic cooling in an optomechanical system consisting of two coupled cantilevers. The hybridization of the cantilevers creates a symmetric mode, which is feedback cooled, and an anti-symmetric mode not directly controllable by the feedback. The scheme of sympathetic cooling is adopted to cool the anti-symmetric mode indirectly by parametrically coupling to the feedback-cooled symmetric mode, from which the cooling power can be transferred. Experiment shows that the realization of coherent dynamics plays an essential role in sympathetic cooling, in which optimal cooling is achieved when the mechanical dissipation rate and the strength of coupling become comparable. The sympathetic cooling is improved by increasing the strength of mode coupling to enhance the transfer of cooling power. Also, the limit of sympathetic cooling imposed by the capacity of feedback cooling is reached as the effective temperatures of the two modes approach the strong coherent coupling condition. Our research provides the prospect of extending the cooling techniques to coupled mechanical resonators for a broad application in sensing and information processing.

KEYWORDS

**sympathetic cooling, optomechanical system, coupled mechanical resonators, coherent coupling, feedback control**

## 1 Introduction

Cooling of the mechanical resonator is of great significance in improving the sensitivity of mechanical sensors [1–6] and a prerequisite for exploring the intriguing quantum phenomena at a macroscale [7–12]. Recent advances on cavity optomechanics that integrates the unique capacity on sensing and controlling mechanical motions have allowed cooling mechanical resonators of different types by means of either laser cooling [13–16] or feedback control [17–21]. For example, the scheme of measurement-based feedback has demonstrated the potential on realizing quantum control of a room-temperature mechanical resonator by developing a sensor capable of resolving the zero-point fluctuation at its thermal decoherence rate [22–24]. With respect to the great successes on cooling of the mechanical resonator, significant efforts have been devoted to scaling up the system by connecting additional mechanical resonators for applications ranging from

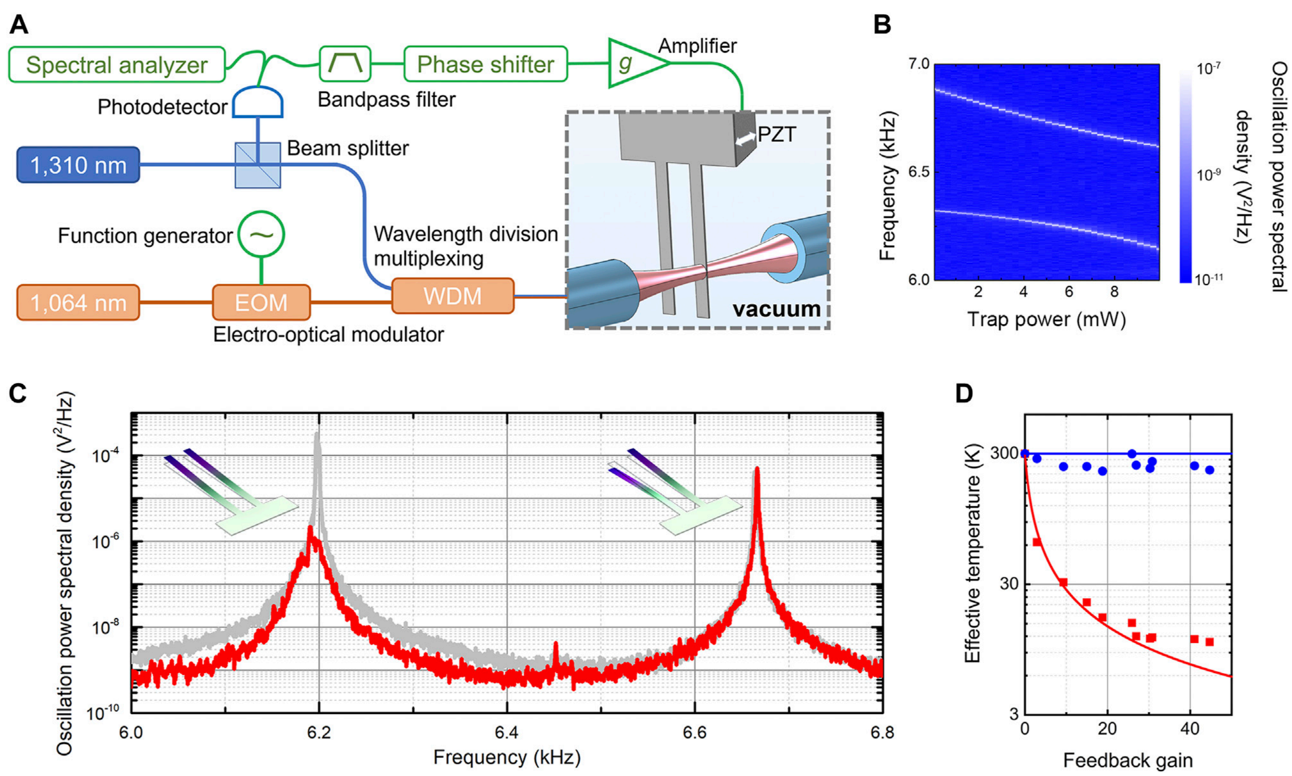


FIGURE 1
**(A)** Schematic illustration of the experimental setup. The power of the 1,310 nm probe is 0.12 mW. A bandpass filter with pass band from 1 kHz to 10 kHz is used to filter out the motion signal of higher-order mechanical modes. Also, the motion signal shifted by a phase of $\pi/2$ is amplified to drive a piezoelectric actuator that shakes the whole chip in the direction parallel to mechanical oscillation to apply the feedback force. The experiment is conducted in high vacuum at an ambient condition with temperature $T_0$ = 300 K. **(B)** Optical mediation of mode hybridization between the two elastically coupled cantilevers. **(C)** Thermal oscillation power spectral density of the elastically coupled cantilevers under the control of feedback. For comparison, the oscillation spectrum at feedback gain $g$ = 9 (red curve) is plotted with that at feedback gain $g$ = 0 (gray curve). Inset: the shapes of oscillation for the symmetric and the anti-symmetric modes. **(D)** Effective temperature of the two normal modes. The effective temperatures of the symmetric mode (red rectangles) and anti-symmetric mode (blue dots) are measured experimentally at different feedback gains. Also, the theoretical results for the symmetric mode (red line) and anti-symmetric mode (blue line) are calculated at the same condition of our experiment.

high-precision measurement [25–27] to scalable phonon-based information processing devices [28–31]. Nevertheless, cooling of coupled mechanical resonators remains a primary obstacle in scaling up the system because the hybridization of mechanical resonators typically creates mechanical modes with shapes that are not directly controllable. Examples include distant mechanical resonators that cannot be addressed by laser [32, 33], optomechanical mode that appears dark to the probe [34, 35], and mechanical modes with symmetries that can balance the actuation force [36].

The realization of cooling in the coupled mechanical resonators beyond that which can be directly cooled would require a controllable coupling between mechanical modes [37–40]. The concept of sympathetic cooling has been achieved in systems such as trapped ions and atoms to cool degrees of freedom that are inaccessible to direct laser cooling [41, 42]. In micro- and nanomechanical systems, coherent coupling between mechanical modes of either distinct mechanical resonators or different modes of the same resonator have been achieved so far by optical [43, 44], electrical [45, 46], and elastic means [47]. Also, dynamical manipulation [48–51], geometric control [52, 53], and topological transfer [54, 55] of mechanical motions have been demonstrated in coupled mechanical resonators. The ability in coherent transfer of motions between the mechanical resonator opens the possibility to sympathetic cooling in coupled mechanical resonators by transferring the cooling power to mechanical modes which is impossible for direct cooling.

In this paper, we present sympathetic feedback cooling in the optomechanical system consisting of two mechanical modes. The scheme of measurement-based feedback is implemented to cool one of the mechanical modes directly. Also, the mechanical mode, which is unable to be actuated by the feedback force due to the symmetry of its oscillation shape, is cooled sympathetically by coupling to the feedback-cooled mode. The coherent dynamics of the sympathetic feedback cooling is investigated by changing the strength of feedback cooling. Also, the strength of mode coupling is enhanced to improve the sympathetic cooling to the limit imposed by the capacity of feedback cooling.

## 2 Methods

The mechanical resonators used in our experiment are two elastically coupled cantilevers with dimensions of 200 μm in length, 10 μm in width, and 200 nm in thickness. As illustrated in Figure 1A, one of the cantilevers (cantilever 1) is inserted into a fiber-based cavity to form a membrane-in-the-middle optomechanical system, in which the cantilever is trapped by a 1,064 nm laser. Consequently, the resonant frequency of cantilever 1 becomes trap power $P$ dependent $\omega_1^2(P) = \omega_1^2(0) + GP$ with $G = -2.02 \times 10^7\ \mathrm{rad^2 s^{-2} mW^{-1}}$ representing the strength of trapping, whereas the frequency of the other cantilever (cantilever 2) $\omega_2$ remains unaffected. In order to monitor the motion of the trapped cantilever, the cavity is pumped by an additional weak 1,310 nm probe, which couples linearly to the motion of cantilever 1. Because of the elastic coupling, the motions of the cantilevers are hybridized into two normal modes in Figure 1B. Specifically, with the frequencies of the cantilevers approaching ($\omega_1 = \omega_2$), an anti-crossing of the mechanical mode can be clearly observed at the trap power of $P_0 = 7.35$ mW with the anti-crossing gap $\Delta/2\pi = 459.5$ Hz. The complete mode hybridization at the avoided crossing point, $\begin{pmatrix} X_s \\ X_a \end{pmatrix} = \frac{1}{\sqrt{2}}\begin{pmatrix} 1 & 1 \\ -1 & 1 \end{pmatrix}\begin{pmatrix} x_1 \\ x_2 \end{pmatrix}$, creates a symmetric mode ($X_s$) and an anti-symmetric mode ($X_a$) with the two cantilevers oscillating in parallel and opposite directions at the same amplitude, respectively. The frequencies of the symmetric and anti-symmetric modes are $\omega_s/2\pi = 6,213.3$ Hz and $\omega_a/2\pi = 6,672.8$ Hz, respectively.

The mechanical resonator is cooled at the anti-crossing point using the scheme of measurement-based feedback, in which a force proportional to the oscillation velocity $F_{\mathrm{fb}}(t) = -mg\gamma_m \dot{x}_1(t)$ is applied with $g$ representing the feedback gain. Although feedback control of different modes simultaneously is possible in its principle, direct feedback cooling of the two modes at the anti-crossing point is complicated as it requires to discriminate the two normal modes that are closely spaced in frequency domain. Here, rather than selectively controlling cantilever 1, we piezoelectrically actuate the whole chip, to which the two cantilevers are connected. Also, the displacement of the $i$th cantilever $x_i$ in the presence of the thermal Brownian force $F_{\mathrm{th},i}$ can be described by

$$\begin{pmatrix} \frac{d^2}{dt^2} + \gamma_m \frac{d}{dt} + \omega_1^2 & -J \\ -J & \frac{d^2}{dt^2} + \gamma_m \frac{d}{dt} + \omega_2^2 \end{pmatrix}\begin{pmatrix} x_1(t) \\ x_2(t) \end{pmatrix} = \frac{1}{m}\begin{pmatrix} F_{\mathrm{fb}}(t) + F_{\mathrm{th},1}(t) \\ F_{\mathrm{fb}}(t) + F_{\mathrm{th},2}(t) \end{pmatrix}, \quad (1)$$

where $J$ denotes the strength of elastic coupling, and the effective mass and the intrinsic damping rate of the two cantilevers are assumed to be nearly identical with $m \approx 1$ ng and $\gamma_m/2\pi \approx 0.22$ Hz, respectively. Owing to the complete hybridization at the anti-crossing point, we find that the feedback force on the $X_a(t)$ can be perfectly balanced. Consequently, in Figure 1C, only the symmetric mode is cold-damped when the feedback is activated, whereas the anti-symmetric mode remains nearly unaffected. The effective damping rate of the symmetric mode, $\gamma_{\mathrm{eff}}^s = (1+g)\gamma_m$, is measured to calibrate the feedback gain. In Figure 1D, the effective temperatures of each mode at different feedback gains are calculated by integrating the spectra in the vicinity of its resonant frequency. Note that measurement noises such as shot noise in the optical detection of mechanical displacement can be amplified by the feedback and influences the motion of mechanical resonator as feedback force noise. When the feedback gain is comparable to $\sqrt{SNR}$ with signal-to-noise ratio in measuring the thermomechanical motion being $SNR = 1.7 \times 10^6$ in our case, the influence of measurement noises can become significant and impose a fundamental limit to measurement-based feedback cooling. For simplicity, the experiments in what follows are conducted at the feedback gain $g \ll \sqrt{SNR}$ so that the influence of the measurement noise is negligible.

# 3 Results and discussion

In order to cool the anti-symmetric mode, a parametric pump is applied to couple the anti-symmetric mode to the feedback-cooled symmetric mode by modulating the trap power $P = P_0 + P_d \cos(\omega_d t)$ with $P_d$ and $\omega_d$ denoting the pump power and pump frequency, respectively. For a high-efficiency sympathetic cooling, the pump frequency is tuned to perfectly compensate the frequency offset between the two modes ($\omega_d = \omega_a - \omega_s$) so that the motions can be resonantly transferred between the two modes by the one-phonon process [49]. Here, by neglecting the contribution of higher-order processes in Equation (1), the motion of the normal mode $X_{a(s)}(t) = \mathrm{Re}[A_{a(s)}(t)\exp(i\omega_{a(s)}t)]$ in the presence of the sympathetic cooling with $A_{a,s}(t)$ denoting the slow-varying complex amplitude of oscillation can be described by

$$\begin{pmatrix} i\frac{d}{dt} + i(1+g)\frac{\gamma_m}{2} & -\frac{\Omega}{2} \\ -\frac{\Omega}{2} & i\frac{d}{dt} + i\frac{\gamma_m}{2} \end{pmatrix}\begin{pmatrix} A_s(t) \\ A_a(t) \end{pmatrix} = \frac{1}{2m\sqrt{2\omega_a\omega_s}}\begin{pmatrix} F_{\mathrm{th},2}(t) + F_{\mathrm{th},1}(t) \\ F_{\mathrm{th},2}(t) - F_{\mathrm{th},1}(t) \end{pmatrix}, \quad (2)$$

with $\Omega = \frac{GP_d}{2\sqrt{\omega_a\omega_s}}$ denoting the strength of parametric coupling [52]. Equation (2) confirms that only the symmetric mode can be cooled by the feedback in the absence of the parametric coupling ($\Omega = 0$). As in Figure 2A, the sympathetic cooling is conducted at the pump power of $P_d = 0.31$ mW. The strength of the parametric coupling which is defined by the normal-mode splitting without feedback cooling ($g = 0$) is $\Omega/2\pi = 4.6$ Hz. In contrast to that without the parametric coupling, the resonance of the anti-symmetric mode is broadened by the feedback, implying that parametric coupling to the feedback-cooled symmetric mode provides an additional energy dissipation channel for the anti-symmetric mode. Also, the effective temperatures of the symmetric mode ($T_{\mathrm{eff}}^s$) and the anti-symmetric mode ($T_{\mathrm{eff}}^a$) are obtained by integrating the areas under the resonances of corresponding modes with

$$T_{\mathrm{eff}}^s = \frac{2\Omega^2 + (2+g)\gamma_m^2}{(2+g)[\Omega^2 + (1+g)\gamma_m^2]}T_0,$$
$$T_{\mathrm{eff}}^a = \frac{2\Omega^2 + (2+g)(1+g)\gamma_m^2}{(2+g)[\Omega^2 + (1+g)\gamma_m^2]}T_0. \quad (3)$$

For a given parametric coupling strength $\Omega \gg \gamma_m$, Eq. (3) indicates that the effective temperature of the anti-symmetric mode can reach its minimal value $T_{\mathrm{eff}}^a \approx \frac{4}{2+g_{\mathrm{opt}}}T_0$ at the optimal feedback gain $g_{\mathrm{opt}} \approx \sqrt{2}\Omega/\gamma_m$. The effective temperatures of the two modes at different feedback gains are plotted in Figure 2B. Indeed, the effective temperature of the anti-symmetric mode is reduced to approximately 30 K as the feedback gain reaches $g = 26$, at which the normal-mode splitting disappears as the effective damping rates of the normal modes becomes comparable to the strength of parametric coupling. The disappearance of the normal-mode

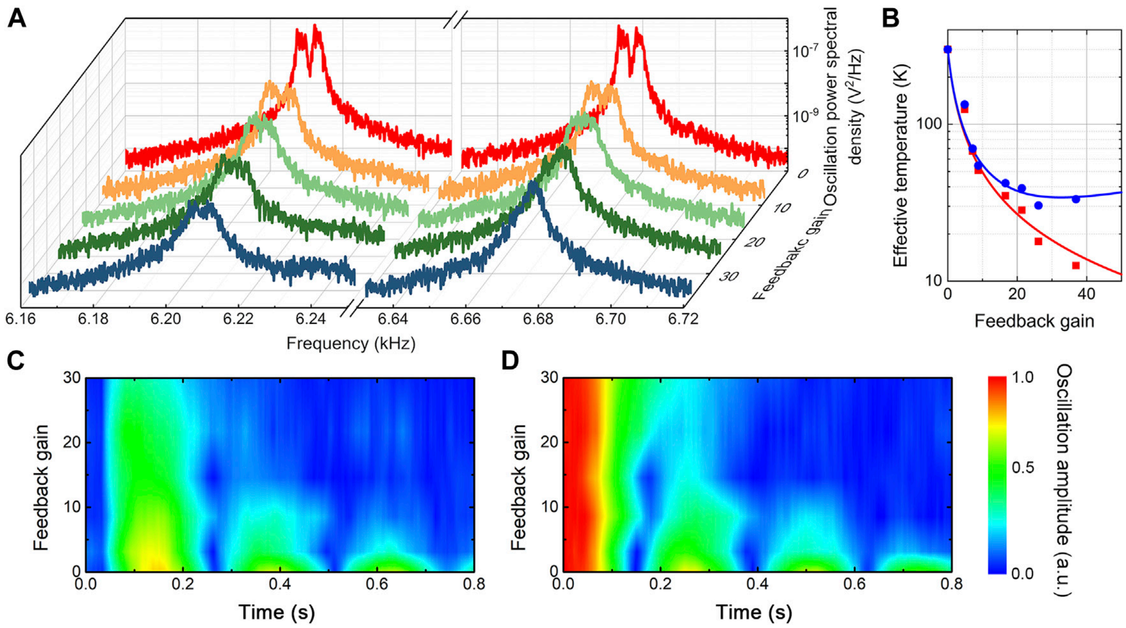


FIGURE 2
**(A)** Thermal oscillation power spectral density of the modes cooled sympathetically at different feedback gains. The spectra for different feedback gains are recorded at the pump power of $P_d$ = 0.31 mW. In the case of $g$ = 0, the parametric pump creates a normal-mode splitting of 4.6 Hz. **(B)** Effective temperature of the modes cooled sympathetically under different feedback gains. The effective temperatures of the symmetric mode (red rectangles) and anti-symmetric mode (blue dots) are measured experimentally by integrating the corresponding spectrum in **(A)** around its resonant frequency. Also, the theoretical results for the symmetric mode (red line) and anti-symmetric mode (blue line) calculated at the same condition of our experiment are plotted for comparison. **(C, D)** Oscillation amplitudes of the symmetric and anti-symmetric modes. The anti-symmetric mode is actuated using the radiation pressure force. Also, the real-time oscillation amplitude is measured experimentally by demodulating the motion signal at the resonant frequencies of the corresponding mode with the bandwidth of 60 Hz.

splitting indicates a transition from strong to weak parametric coupling between the two modes. By increasing the feedback gain further, the effective temperature of the anti-symmetric mode starts to rise although the symmetric mode can be cooled continuously.

The dependence of the optimal feedback gain on the parametric coupling strength reveals that the coherent dynamics plays an essential role in transferring the cooling power between the parametrically coupled modes. The real-time dynamics of the motion transduction is investigated by initializing the system through resonantly actuating the anti-symmetric mode to an oscillation amplitude of approximately 50 nm. After the initialization, the parametric pump with $P_d = 0.31\,\mathrm{mW}$ is applied immediately to couple the anti-symmetric mode to the feedback-cooled symmetric mode. In Figures 2C,D, the oscillation amplitudes of the two modes $|A_{a,s}(t)|$ are recorded in the duration that the parametric pump is applied. At the feedback gain $g = 0$, the motions on the two modes can be coherently exchanged through the Rabi-like oscillation at the frequency of 4.3 Hz, which is in good agreement with the normal-mode splitting $\Omega/2\pi = 4.6\,\mathrm{Hz}$ observed in Figure 2A. However, when the feedback gain exceeds $g = 20$, the mechanical motions can no longer be coherently exchanged between the two modes before decaying out, confirming that the two modes are weakly coupled. Also, in the weak coupling regime, it is interesting that the energy dissipation rate for the anti-symmetric mode decreases as the feedback gain increases although the symmetric mode can be further damped. Such difference reflects that the stronger feedback cooling of the symmetric mode is counterbalanced by a weaker energy transduction, which leads to the optimal sympathetic cooling of anti-symmetric mode observed in Figure 2B.

We demonstrate that sympathetic cooling can be improved by increasing the strength of parametric coupling to enhance the transfer of cooling power. The strength of parametric coupling for each pump power $P_d$ is calibrated at $g = 0$ by measuring the normal-mode splitting $\Omega$ with $d\Omega/dP_d \approx 2\pi \times 14.7\,\mathrm{rad}\cdot\mathrm{s}^{-1}\mathrm{mW}^{-1}$. As in Figure 3A, the anti-symmetric mode is sympathetically cooled by parametrically coupling to the symmetric mode, which is feedback-cooled at a fixed gain $g = 25$. It shows that the sympathetic cooling can be improved obviously by turning up the parametric pump. As the pump power beyond $P_d = 0.57\,\mathrm{mW}$, a strong parametric coupling between the anti-symmetric mode and the feedback-cooled symmetric mode is achieved, which creates a clear normal-mode splitting. The effective temperatures of the two modes at different parametric coupling strengths are plotted in Figure 3B. The transfer of cooling power between the two modes reduces the effective temperature of the anti-symmetric mode at the expense of heating up the symmetric mode at the mean time. Also, the limit of the sympathetic cooling imposed by the cooling capacity of feedback is reached as the effective temperatures of the two modes approaching $T_{\mathrm{eff}}^{a,s} \to \frac{2}{2+g}T_0$ at the condition of strong parametric pump ($\Omega \gg g\gamma_m$). In our experiment, sympathetic cooling of the anti-symmetric mode close to the limit with $T_{\mathrm{eff}}^{a} = 27\,\mathrm{K}$ is achieved at the pump power of $P_d = 0.77\,\mathrm{mW}$ with the effective temperature of the feedback-cooled symmetric mode rising from 15 K to 25 K.

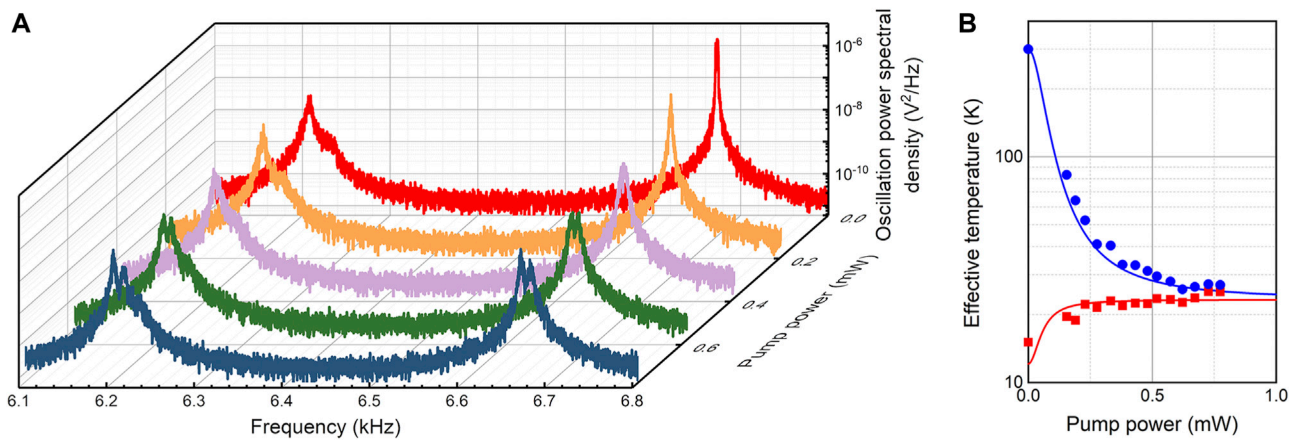


FIGURE 3
**(A)** Thermal oscillation power spectral density of the modes cooled sympathetically at different pump powers. The spectra for different pump powers are recorded at the feedback gain of $g$ = 25. **(B)** Effective temperature of the two modes cooled sympathetically under different pump powers. The effective temperatures of the symmetric mode (red rectangles) and the anti-symmetric mode (blue dots) are measured experimentally by integrating the corresponding spectrum in **(A)** around its resonant frequency. Also, the theoretical results for the symmetric mode (red line) and anti-symmetric mode (blue line) calculated at the same condition of our experiment are plotted for comparison.

# 4 Conclusion

In summary, we have presented sympathetic feedback cooling of elastically coupled mechanical resonators in an optomechanical system, which allows for sensing and coherent controlling of mechanical motions simultaneously. The complete hybridization between cantilevers creates two normal modes with the cantilevers oscillating symmetrically and anti-symmetrically. In order to cool the anti-symmetric mode that is beyond direct control due to its oscillation shape, a parametric pump is applied to resonantly couple the two modes. As a result, when the symmetric mode is feedback cooled, the cooling power can be transferred to the anti-symmetric mode. We demonstrate that the coherent dynamics plays an essential role in sympathetic cooling with an optimal cooling achieved when the mechanical dissipation becomes comparable to the strength of parametric coupling. The sympathetic cooling is improved by increasing the strength of parametric coupling to enhance the transfer of cooling power. Also, sympathetic cooling of the anti-symmetric mode to the limit imposed by the capacity of feedback is achieved when the effective temperatures of the two modes approach.

Although the sympathetic cooling of the anti-symmetric mode, which has been widely adopted in mechanical sensors for its resilience to vibration noises [36, 56–58], is demonstrated in our experiment, the scheme can be generally extended to coupled mechanical resonator array to transfer cooling power to distant mechanical resonators that are inaccessible by direct cooling. Also, significant improvement on the limit of sympathetic cooling can be expected under the condition of deep feedback cooling, in which the measurement noises, such as shot noise and photodetector noise, should be taken into account. With respect to the great advances on the measurement-based feedback control, our research on sympathetic feedback cooling provides a feasible scheme to cool coupled mechanical resonators for scalable phonon information processing.

# Data availability statement

The raw data supporting the conclusion of this article will be made available by the authors, without undue reservation.

# Author contributions

HF and Z-CG designed and conceived the experiment. C-YS, Z-CG, and QY carried out the measurements. C-YS proceeded and analyzed the experimental data. YL provided theoretical support. HF and YL wrote the paper. C-PS and HF supervised the project. All authors contributed to the article and approved the submitted version.

# Funding

This work was supported by the National Natural Science Foundation of China (grant nos. U2130117, 12074030, 12274107, U1930403, U1930402, and 12088101), the Natural Science Foundation of Hubei Province (grant no. 2020CFB830), and the Research Funds of Hainan University [grant no. KYQD (ZR) 22170].

# Acknowledgments

Z-CG gratefully acknowledges the helpful discussion with Jie-qiao Liao at Hunan Normal University.

# Conflict of interest

The authors declare that the research was conducted in the absence of any commercial or financial relationships that could be construed as a potential conflict of interest.

## Publisher's note

All claims expressed in this article are solely those of the authors and do not necessarily represent those of their affiliated organizations, or those of the publisher, the editors, and the reviewers. Any product that may be evaluated in this article, or claim that may be made by its manufacturer, is not guaranteed or endorsed by the publisher.

## References


1. Chen Y. Macroscopic quantum mechanics: Theory and experimental concepts of optomechanics. *J Phys B-at Mol Opt* (2013) 46(10):104001. doi:10.1088/0953-4075/46/10/104001

2. Lei CU, Weinstein AJ, Suh J, Wollman EE, Kronwald A, Marquardt F, et al. Quantum nondemolition measurement of a quantum squeezed state beyond the 3 dB limit. *Phys Rev Lett* (2016) 117(10):100801. doi:10.1103/PhysRevLett.117.100801

3. Miao H, Srinivasan K, Aksyuk V. A microelectromechanically controlled cavity optomechanical sensing system. *New J Phys* (2012) 14(7):075015. doi:10.1088/1367-2630/14/7/075015

4. Yi S, Xiang J, Zhou M, Wu Z, Yang L, Yu Z. Angle-based wavefront sensing enabled by the near fields of flat optics. *Nat Commun* (2021) 12(1):6002. doi:10.1038/s41467-021-26169-z

5. Jiang X, Qavi AJ, Huang SH, Yang L. Whispering-gallery sensors. *Matter* (2020) 3(2):371–92. doi:10.1016/j.matt.2020.07.008

6. Tang SJ, Liu S, Yu XC, Song Q, Gong Q, Xiao YF. On-chip spiral waveguides for ultrasensitive and rapid detection of nanoscale objects. *Adv Mater* (2018) 30(25): e1800262. doi:10.1002/adma.201800262

7. Aspelmeyer M, Kippenberg TJ, Marquardt F. Cavity optomechanics. *Rev Mod Phys* (2014) 86(4):1391–452. doi:10.1103/RevModPhys.86.1391

8. Barzanjeh S, Redchenko ES, Peruzzo M, Wulf M, Lewis DP, Arnold G, et al. Stationary entangled radiation from micromechanical motion. *Nature* (2019) 570(7762):480–3. doi:10.1038/s41586-019-1320-2

9. Safavi-Naeini AH, Chan J, Hill JT, Alegre TP, Krause A, Painter O. Observation of quantum motion of a nanomechanical resonator. *Phys Rev Lett* (2012) 108(3):033602. doi:10.1103/PhysRevLett.108.033602

10. Ockeloen-Korppi CF, Damskagg E, Pirkkalainen JM, Asjad M, Clerk AA, Massel F, et al. Stabilized entanglement of massive mechanical oscillators. *Nature* (2018) 556(7702):478–82. doi:10.1038/s41586-018-0038-x

11. Poot M, van der Zant HSJ. Mechanical systems in the quantum regime. *Phys Rep* (2012) 511(5):273–335. doi:10.1016/j.physrep.2011.12.004

12. Riedinger R, Hong S, Norte RA, Slater JA, Shang J, Krause AG, et al. Non-classical correlations between single photons and phonons from a mechanical oscillator. *Nature* (2016) 530(7590):313–6. doi:10.1038/nature16536

13. Chan J, Alegre TP, Safavi-Naeini AH, Hill JT, Krause A, Groblacher S, et al. Laser cooling of a nanomechanical oscillator into its quantum ground state. *Nature* (2011) 478(7367):89–92. doi:10.1038/nature10461

14. Qiu L, Shomroni I, Seidler P, Kippenberg TJ. Laser cooling of a nanomechanical oscillator to its zero-point energy. *Phys Rev Lett* (2020) 124(17):173601. doi:10.1103/PhysRevLett.124.173601

15. Teufel JD, Donner T, Li D, Harlow JW, Allman MS, Cicak K, et al. Sideband cooling of micromechanical motion to the quantum ground state. *Nature* (2011) 475(7356):359–63. doi:10.1038/nature10261

16. Clark JB, Lecocq F, Simmonds RW, Aumentado J, Teufel JD. Sideband cooling beyond the quantum backaction limit with squeezed light. *Nature* (2017) 541(7636): 191–5. doi:10.1038/nature20604

17. Kleckner D, Bouwmeester D. Sub-kelvin optical cooling of a micromechanical resonator. *Nature* (2006) 444(7115):75–8. doi:10.1038/nature05231

18. Poggio M, Degen CL, Mamin HJ, Rugar D. Feedback cooling of a cantilever's fundamental mode below 5 mK. *Phys Rev Lett* (2007) 99(1):017201. doi:10.1103/PhysRevLett.99.017201

19. Schmid G-L, Ngai CT, Ernzer M, Aguilera MB, Karg TM, Treutlein P. Coherent feedback cooling of a nanomechanical membrane with atomic spins. *Phys Rev X* (2022) 12(1):011020. doi:10.1103/PhysRevX.12.011020

20. Zhang J, Liu Y, Wu RB, Jacobs K, Nori F. Quantum feedback: Theory, experiments, and applications. *Phys Rep* (2017) 679(17):1–60. doi:10.1016/j.physrep.2017.02.003

21. Schafermeier C, Kerdoncuff H, Hoff UB, Fu H, Huck A, Bilek J, et al. Quantum enhanced feedback cooling of a mechanical oscillator using nonclassical light. *Nat Commun* (2016) 7:13628. doi:10.1038/ncomms13628

22. Guo J, Norte R, Groblacher S. Feedback cooling of a room temperature mechanical oscillator close to its motional ground state. *Phys Rev Lett* (2019) 123(22):223602. doi:10.1103/PhysRevLett.123.223602

23. Wilson DJ, Sudhir V, Piro N, Schilling R, Ghadimi A, Kippenberg TJ. Measurement-based control of a mechanical oscillator at its thermal decoherence rate. *Nature* (2015) 524(7565):325–9. doi:10.1038/nature14672

24. Rossi M, Mason D, Chen J, Tsaturyan Y, Schliesser A. Measurement-based quantum control of mechanical motion. *Nature* (2018) 563(7729):53–8. doi:10.1038/s41586-018-0643-8

25. Lin Y, Yabuno H, Liu X, Yamamoto Y, Matsumoto S. Highly sensitive AFM using self-excited weakly coupled cantilevers. *Appl Phys Lett* (2019) 115(13):133105. doi:10.1063/1.5115836

26. Manav M, Phani AS, Cretu E. Mode localized MEMS transducers with voltage-controlled linear coupling. *J Micromech Microeng* (2017) 27(5):055010. doi:10.1088/1361-6439/aa6652

27. Marquez S, Alvarez M, Plaza JA, Villanueva LG, Dominguez C, Lechuga LM. Asymmetrically coupled resonators for mass sensing. *Appl Phys Lett* (2017) 111(11): 113101. doi:10.1063/1.5003023

28. Habraken SJM, Stannigel K, Lukin MD, Zoller P, Rabl P. Continuous mode cooling and phonon routers for phononic quantum networks. *New J Phys* (2012) 14(11): 115004. doi:10.1088/1367-2630/14/11/115004

29. Fu H, Gong ZC, Yang LP, Mao TH, Sun CP, Yi S, et al. Coherent optomechanical switch for motion transduction based on dynamically localized mechanical modes. *Phys Rev Appl* (2018) 9(5):054024. doi:10.1103/PhysRevApplied.9.054024

30. Barzanjeh S, Wulf M, Peruzzo M, Kalaee M, Dieterle PB, Painter O, et al. Mechanical on-chip microwave circulator. *Nat Commun* (2017) 8(1):953. doi:10.1038/s41467-017-01304-x

31. Huang P, Zhang L, Zhou J, Tian T, Yin P, Duan C, et al. Nonreciprocal radio frequency transduction in a parametric mechanical artificial lattice. *Phys Rev Lett* (2016) 117(1):017701. doi:10.1103/PhysRevLett.117.017701

32. Luo G, Zhang ZZ, Deng GW, Li HO, Cao G, Xiao M, et al. Strong indirect coupling between graphene-based mechanical resonators via a phonon cavity. *Nat Commun* (2018) 9(1):383. doi:10.1038/s41467-018-02854-4

33. Lin S, Tian T, Huang P, Yin P, Zhang L, Du J. Realization of programmable nanomechanical lattice with both nearest-neighboring and next-nearest-neighboring couplings. *Appl Phys Lett* (2020) 117(9):093503. doi:10.1063/5.0009302

34. Dong C, Fiore V, Kuzyk MC, Wang H. Optomechanical dark mode. *Science* (2012) 338(6114):1609–13. doi:10.1126/science.1228370

35. Wang Y-D, Clerk AA. Using dark modes for high-fidelity optomechanical quantum state transfer. *New J Phys* (2012) 14(10):105010. doi:10.1088/1367-2630/14/10/105010

36. Pachkawade V. State-of-the-Art in mode-localized mems coupled resonant sensors: A comprehensive review. *IEEE Sens J* (2021) 21(7):8751–79. doi:10.1109/JSEN.2021.3051240

37. Frimmer M, Gieseler J, Novotny L. Cooling mechanical oscillators by coherent control. *Phys Rev Lett* (2016) 117(16):163601. doi:10.1103/PhysRevLett.117.163601

38. Lai DG, Huang J, Hou BP, Nori F, Liao JQ. Domino cooling of a coupled mechanical-resonator chain via cold-damping feedback. *Phys Rev A* (2021) 103(6): 063509. doi:10.1103/PhysRevA.103.063509

39. Lai DG, Zou F, Hou BP, Xiao YF, Liao JQ. Simultaneous cooling of coupled mechanical resonators in cavity optomechanics. *Phys Rev A* (2018) 98(2):023860. doi:10.1103/PhysRevA.98.023860

40. Jockel A, Faber A, Kampschulte T, Korppi M, Rakher MT, Treutlein P. Sympathetic cooling of a membrane oscillator in a hybrid mechanical-atomic system. *Nat Nanotechnol* (2015) 10(1):55–9. doi:10.1038/nnano.2014.278

41. Bohman M, Grunhofer V, Smorra C, Wiesinger M, Will C, Borchert MJ, et al. Sympathetic cooling of a trapped proton mediated by an LC circuit. *Nature* (2021) 596(7873):514–8. doi:10.1038/s41586-021-03784-w

42. Christoph P, Wagner T, Zhong H, Wiesendanger R, Sengstock K, Schwarz A, et al. Combined feedback and sympathetic cooling of a mechanical oscillator coupled to ultracold atoms. *New J Phys* (2018) 20(9):093020. doi:10.1088/1367-2630/aadf20

43. Lin Q, Rosenberg J, Chang D, Camacho R, Eichenfield M, Vahala KJ, et al. Coherent mixing of mechanical excitations in nano-optomechanical structures. *Nat Photon* (2010) 4(4):236–42. doi:10.1038/nphoton.2010.5

44. Shkarin AB, Flowers-Jacobs NE, Hoch SW, Kashkanova AD, Deutsch C, Reichel J, et al. Optically mediated hybridization between two mechanical modes. *Phys Rev Lett* (2014) 112(1):013602. doi:10.1103/PhysRevLett.112.013602

45. Huang P, Wang P, Zhou J, Wang Z, Ju C, Wang Z, et al. Demonstration of motion transduction based on parametrically coupled mechanical resonators. *Phys Rev Lett* (2013) 110(22):227202. doi:10.1103/PhysRevLett.110.227202

46. Okamoto H, Schilling R, Schütz H, Sudhir V, Wilson DJ, Yamaguchi H, et al. A strongly coupled Λ-type micromechanical system. *Appl Phys Lett* (2016) 108(15): 153105. doi:10.1063/1.4945741

47. Gong ZC, Fu H, Mao TH, Yuan Q, Shen CY, Sun CP, et al. Coherent phonon-mediated dynamics for an addressable transducer of coupled micro-mechanical resonators. *Appl Phys Lett* (2021) 118(20):203505. doi:10.1063/5.0044428

48. Faust T, Rieger J, Seitner MJ, Kotthaus JP, Weig EM. Coherent control of a classical nanomechanical two-level system. *Nat Phys* (2013) 9(8):485–8. doi:10.1038/nphys2666

49. Okamoto H, Gourgout A, Chang C-Y, Onomitsu K, Mahboob I, Chang EY, et al. Coherent phonon manipulation in coupled mechanical resonators. *Nat Phys* (2013) 9(8):480–4. doi:10.1038/nphys2665

50. Fu H, Gong ZC, Mao TH, Sun CP, Yi S, Li Y, et al. Classical analog of Stückelberg interferometry in a two-coupled-cantilever–based optomechanical system. *Phys Rev A* (2016) 94(4):043855. doi:10.1103/PhysRevA.94.043855

51. Zhang Z-Z, Song X-X, Luo G, Su Z-J, Wang K-L, Cao G, et al. Coherent phonon dynamics in spatially separated graphene mechanical resonators. *P Natl Acad Sci USA* (2020) 117(11):5582–7. doi:10.1073/pnas.1916978117

52. Fu H, Gong ZC, Mao TH, Shen CY, Sun CP, Yi S, et al. Geometric energy transfer in a stückelberg interferometer of two parametrically coupled mechanical modes. *Phys Rev Appl* (2019) 11(3):034010. doi:10.1103/PhysRevApplied.11.034010

53. Yuan Q, Gong ZC, Gao YZ, Mao TH, Shen CY, Sun CP, et al. Geometric motion transfer between two indirectly coupled mechanical resonators. *Appl Phys Lett* (2021) 119(14):143504. doi:10.1063/5.0060300

54. Xu H, Mason D, Jiang L, Harris JG. Topological energy transfer in an optomechanical system with exceptional points. *Nature* (2016) 537(7618):80–3. doi:10.1038/nature18604

55. Xu H, Jiang L, Clerk AA, Harris JGE. Nonreciprocal control and cooling of phonon modes in an optomechanical system. *Nature* (2019) 568(7750):65–9. doi:10.1038/s41586-019-1061-2

56. Giner J, Zhang Y, Maeda D, Ono K, Shkel AM, Sekiguchi T. Dynamicaly balanced degenerate mode gyro with sub-hz frequency symmetry and temperature robustness. In: 2017 IEEE 30th International Conference on Micro Electro Mechanical Systems (MEMS); 22-26 January 2017; Las Vegas (2017).

57. Senkal D, Efimovskaya A, Shkel AM. Miniature origami-like folded MEMS TIMU. In: 2015 IEEE International Symposium on Inertial Sensors and Systems (ISISS) Proceedings; 21-25 June 2015; Anchorage (2015).

58. Trusov AA, Schofield AR, Shkel AM. Gyroscope architecture with structurally forced anti-phase drive-mode and linearly coupled anti-phase sense-mode. In: TRANSDUCERS 2009 - 2009 International Solid-State Sensors, Actuators and Microsystems Conference; 21-25 June 2009; Denver (2009).